Electronic and magnetic structures of cuprates with spin-orbit interaction

W. Koshibae, Y. Ohta, and S. Maekawa
Department of Applied Physics, Nagoya University, Nagoya 464-01, Japan
(Received 14 April 1992; revised manuscript received 20 October 1992)

The effective Hamiltonian for the CuO_2 plane of high-T_c cuprates is derived by taking into account the spin-orbit interaction. A finite-size exact-diagonalization technique is applied to the Hamiltonian, and the magnetic and electronic structures of the CuO_2 plane in the low-temperature orthorhombic (LTO) and low-temperature tetragonal (LTT) phases of the La_2CuO_4-type crystals are examined. It is shown that the contribution from the in-plane oxygen $2p_z$ orbital perpendicular to the plane is essential for the emergence of the weak ferromagnetism in the LTO-phase La_2CuO_4. In the LTT phase, either the uniaxial antiferromagnetism or the weak ferromagnetism is induced, depending on how the $2p_z$ orbital contributes to the anisotropic superexchange interaction of the single Cu–O–Cu bond. We study the dynamics of a hole in an extended t-J model, and show that the lattice distortion works to change the symmetry of the electronic ground state via the spin-orbit coupling. The effect is, however, small and seems irrelevant to the anomalous properties of $La_{1.88}Ba_{0.12}CuO_4$.

I. INTRODUCTION

The La_2CuO_4-type compounds such as $La_{2-x}Sr_xCuO_4$, $La_{2-x}Ba_xCuO_4$,[1] and $La_{1.6-x}Nd_{0.4}Sr_xCuO_4$ (Ref. 2) exhibit a number of crystal structures including the high-temperature tetragonal (HTT) phase, the low-temperature orthorhombic (LTO) phase, and the low-temperature tetragonal (LTT) phase. Depending on the crystal structures, the compounds show various electronic and magnetic properties, which are of particular interest in relation to emergence of the high-T_c superconductivity of cuprates. Undoped La_2CuO_4 shows weak ferromagnetism in the LTO phase,[3] for which the Dzyaloshinski-Moriya (DM) interaction[4,5] in the CuO_2 plane is responsible. $La_{2-x}Ba_xCuO_4$ shows anomalous behaviors of both the normal-state transport and superconducting properties at a doping rate of $x \simeq 0.12$,[6–9] which is accompanied by a structural phase transition into the LTT phase. A magnetic ordering has been found in this phase.[10,11] It has also been reported[12] that the disappearance of superconductivity in overdoped $La_{2-x}Sr_xCuO_4$ is associated with the LTO-HTT structural phase transition. These experimental facts indicate that the magnetic, normal-state transport, and superconducting properties of the cuprates have an intriguing coupling with the distortion of the lattice structure of the CuO_2 plane. To clarify the nature of the coupling is obviously very important and may provide a key to understand the mechanism of the high-T_c superconductivity of the cuprates.

One of such couplings proposed so far is the DM interaction. The DM interaction, which arises from a mixture of superexchange and spin-orbit coupling under distorted lattices, was first studied to find the origin of the weak ferromagnetism of LTO-phase La_2CuO_4. Coffey, Bedell, and Trugman[13] have correctly described the structure of the DM interaction in the CuO_2 plane from symmetry arguments for the first time. Coffey, Rice, and Zhang[14] then used the perturbation theory of Moriya[5] and claimed that the obtained DM interaction in the CuO_2 plane has the structure of various patterns and in some cases causes the weak-ferromagnetic component in ordered antiferromagnetic Cu spins. Bonesteel, Rice, and Zhang[15] have further claimed that the spin-orbit coupling of the type responsible for the DM interaction can result in a stabilization of a commensurate antiferromagnetic state over a spiral state in the presence of a sufficiently large tilt distortion in the doped CuO_2 plane and argued that the effect may be the origin of the anomalous properties of $La_{1.88}Ba_{0.12}CuO_4$. Recently, Shekhtman, Entin-Wohlman, and Aharony[16] have pointed out the importance of the pseudodipolar term (higher-order spin-orbit coupling term). The work of previous authors[5,13–15,17] has not fully recognized its role. Shekhtman, Entin-Wohlman, and Aharony[16] claimed that the exchange interaction of a single bond derived by Moriya[5] is in fact isotropic and that the frustration due to the noncolinear structure of the DM interaction is essential for the emergence of weak ferromagnetism. Bonesteel[18] has discussed the magnetism of $YBa_2Cu_3O_6$ as well.

In this paper we derive the effective Hamiltonian for the CuO_2 plane in the LTO and LTT phases of La_2CuO_4-type crystals, by taking into account the spin-orbit coupling, and study the effects of lattice distortions on the magnetic and electronic structures of the CuO_2 plane. The proposal of Shekhtman, Entin-Wohlman, and Aharony[16] for weak ferromagnetism is thereby reexamined. The exact-diagonalization technique for finite-size systems is then used to obtain the eigenstates of the Hamiltonian, and some correlation functions for the ground and excited states are evaluated. The results given by Coffey, Rice, and Zhang[14] and Bonesteel, Rice, and Zhang[15] are thereby reexamined.

In Sec. II we apply the perturbation theory of Moriya[5] to the CuO_2 plane and obtain the effective spin Hamiltonian in the LTO and LTT phases. The Hamiltonian consists of the Heisenberg exchange, DM, and pseudodipolar interactions. We show that a subtle balance of con-

tributions from the orbitals on the oxygen ion determines the anisotropic superexchange interaction between two spins of the neighboring Cu ions. The contributions from the oxygen $2p_z$ orbital appearing due to lattice distortions are essential for understanding the magnetism induced by the spin-orbit interaction. The single-band model[16] is not sufficient when one discusses the anisotropy of the magnetism.

In Sec. III we apply the exact-diagonalization technique for finite-size lattices to the obtained effective Hamiltonian for the undoped CuO_2 plane and discuss the magnetism of the plane. We show that, in the LTO phase of La_2CuO_4, the contribution from the $2p_z$ orbital of the in-plane oxygen ions is essential for the emergence of weak ferromagnetism. In the LTT phase of La_2CuO_4-type crystals, either weak ferromagnetism or uniaxial antiferromagnetism is shown to be induced, depending on how the oxygen $2p_z$ orbital contributes to the anisotropic superexchange interaction of the single Cu–O–Cu bond. The frustration among different bonds[16] need not be put forward for discussing weak ferromagnetism.

In Sec. IV we study the effect of the spin-orbit interaction on the dynamics of a hole in an extended t-J model by using the exact-diagonalization technique. We show that the symmetry of the electronic ground state changes due to the lattice distortion via the spin-orbit interaction. The change appears most strongly in the case where the uniaxial antiferromagnetism is stabilized in the undoped phase. This effect is, however, small in the realistic parameter region; we do not think that the effect may be the origin of the anomalous properties of $La_{1.88}Ba_{0.12}CuO_4$.

Conclusions are given in Sec. V. We have reported some preliminary results given in Sec. III elsewhere.[17]

II. DZYALOSHINSKI-MORIYA INTERACTION

In this section we derive the DM interaction in the CuO_2 plane by following the perturbation theory of Moriya.[5] The Hamiltonian for the CuO_2 plane with spin-orbit interaction is written as a sum of the on-site, hopping, and spin-orbit terms:

$$H = H_0 + H_t + H_{LS} , \tag{1}$$

where

$$H_0 = \sum_{jm\sigma} \varepsilon_m d^\dagger_{jm\sigma} d_{jm\sigma} + \sum_{kn\sigma} \varepsilon_{p_n} p^\dagger_{kn\sigma} p_{kn\sigma} + U \sum_{jmm'} d^\dagger_{jm\uparrow} d^\dagger_{jm'\downarrow} d_{jm'\downarrow} d_{jm\uparrow} , \tag{2}$$

$$H_t = \sum_{jm\sigma} \sum_{k(j)n} (t_{jm,kn} d^\dagger_{jm\sigma} p_{kn\sigma} + \text{H.c.}) , \tag{3}$$

and

$$H_{LS} = \lambda \sum_j \mathbf{L}_j \cdot \mathbf{S}_j . \tag{4}$$

$k(j)$ denotes the oxygen site of the neighboring Cu site j, $d^\dagger_{jm\sigma}$ is the creation operator of a hole with spin σ on the mth $3d$ orbital of the jth Cu ion, ε_m is the energy of the mth $3d$ orbital, $p^\dagger_{kn\sigma}$ is the creation operator of a hole on the $2p_n$ orbital ($n = x$, y, and z) of the kth oxygen ion, and ε_{p_n} is the energy of the $2p_n$ orbital. The energies are measured from the lowest-energy level of the Cu $3d$ orbitals, and U is the Coulomb interaction constant between holes on the Cu site. We assume that U is independent of the orbitals. $t_{jm,kn}$ denotes the transfer of a hole between the mth orbital of the Cu ion j and one of the $2p_n$ orbitals of the neighboring O ions k; note that a number of nonzero $t_{jm,kn}$ values appear due to lattice distortions. $\mathbf{L}_j$ and $\mathbf{S}_j$ denote the orbital and spin angular momenta at the j site, respectively, and λ is the spin-orbit coupling constant of the Cu ion.

Let us apply perturbation theory. In the first order of λ, we obtain the following Hamiltonian by eliminating the excited crystal-field levels of Eq. (1):

$$H = \sum_{kn\sigma} \varepsilon_{p_n} p^\dagger_{kn\sigma} p_{kn\sigma} + U \sum_j d^\dagger_{j0\uparrow} d^\dagger_{j0\downarrow} d_{j0\downarrow} d_{j0\uparrow} + \sum_{jk(j)n} \sum_\sigma (t_{j0,kn} d^\dagger_{j0\sigma} p_{kn\sigma} + \text{H.c.}) + \sum_{jk(j)n} \sum_{\alpha\beta} [\mathbf{C}_{jkn} \cdot (d^\dagger_{j0\alpha} \boldsymbol{\sigma}_{\alpha\beta} p_{kn\beta}) + \text{H.c.}] , \tag{5}$$

with

$$\mathbf{C}_{jkn} = -\frac{\lambda}{2} \sum_m \frac{\mathbf{L}^*_{jm0}}{\varepsilon_m} t_{jm,kn} , \tag{6}$$

where $\boldsymbol{\sigma}_{\alpha\beta}$ is the Pauli spin matrix and $\mathbf{L}^*_{jm0}$ is the complex conjugate of the matrix element of $\mathbf{L}_j$ between the mth and ground states of the jth Cu ion. Examining the fourth-order terms with respect to the transfer parameter $t_{jm,kn}$ in perturbation theory, we find the following Hamiltonian with the effective superexchange interaction between the neighboring spins on the Cu ions $\mathbf{S}_i$ and $\mathbf{S}_j$:

$$H_{\text{ex}} = J \sum_{\langle ij \rangle} \mathbf{S}_i \cdot \mathbf{S}_j + \sum_{\langle ij \rangle} \mathbf{D}_{ij} \cdot (\mathbf{S}_i \times \mathbf{S}_j) + \sum_{\langle ij \rangle} \mathbf{S}_i \overleftrightarrow{\Gamma}_{ij} \mathbf{S}_j , \tag{7}$$

with

$$J = 4 \sum_{nn'} (t_{i0,kn} t_{kn,j0} + \mathbf{C}_{i,kn} \cdot \mathbf{C}_{kn,j}) g_{nn'} (t_{j0,kn'} t_{kn',i0} + \mathbf{C}_{j,kn'} \cdot \mathbf{C}_{kn',i}) , \tag{8}$$

$$\mathbf{D}_{ij} = -4i \sum_{nn'} [(\mathbf{C}_{i,kn} t_{kn,j0} + t_{i0,kn} \mathbf{C}_{kn,j}) g_{nn'} (t_{j0,kn'} t_{kn',i0} + \mathbf{C}_{j,kn'} \cdot \mathbf{C}_{kn',i}) - (t_{i0,kn} t_{kn,j0} + \mathbf{C}_{i,kn} \cdot \mathbf{C}_{kn,j}) g_{nn'} (\mathbf{C}_{j,kn'} t_{kn',i0} + t_{j0,kn'} \mathbf{C}_{kn',i})] , \tag{9}$$

and

$$\vec{\Gamma}_{ij}=4\sum_{nn'}\{(\overleftarrow{\mathbf{C}}_{ikn}t_{kn,j0}+t_{i0,kn}\overleftarrow{\mathbf{C}}_{knj})g_{nn'}(\vec{\mathbf{C}}_{jkn'}t_{kn',i0}+t_{j0,kn'}\vec{\mathbf{C}}_{kn'i})+(\overleftarrow{\mathbf{C}}_{jkn}t_{kn,i0}+t_{j0,kn}\overleftarrow{\mathbf{C}}_{kni})g_{nn'}(\vec{\mathbf{C}}_{ikn'}t_{kn',j0}+t_{i0,kn'}\vec{\mathbf{C}}_{kn'j})$$
$$-\overleftrightarrow{1}[(\mathbf{C}_{ikn}t_{kn,j0}+t_{i0,kn}\mathbf{C}_{knj})g_{nn'}(\mathbf{C}_{jkn'}t_{kn',i0}+t_{j0,kn'}\mathbf{C}_{kn'i})]\}\ . \tag{10}$$

The vector with the arrow $\leftarrow$ or $\rightarrow$ indicates that the inner product is taken with the spin operator put in the direction of the arrow. $\overleftrightarrow{1}$ is a 3×3 unit matrix. $g_{nn'}$ is given by

$$g_{nn'}=\begin{cases}\dfrac{1}{\varepsilon_{p_n}^2}\left[\dfrac{1}{U}+\dfrac{1}{2\varepsilon_{p_n}}\right] & (n=n')\ ,\\ \dfrac{1}{\varepsilon_{p_n}\varepsilon_{p_{n'}}}\dfrac{1}{U}+\left[\dfrac{1}{\varepsilon_{p_n}}+\dfrac{1}{\varepsilon_{p_{n'}}}\right]^2\dfrac{1}{\varepsilon_{p_n}+\varepsilon_{p_{n'}}} & (n\neq n')\ .\end{cases} \tag{11}$$

The CuO_2 planes of La_2CuO_4-type crystals are illustrated in Figs. 1 and 2. In the LTO phase, the CuO_6 octahedra rotate alternately about the $\langle 1\bar{1}0\rangle$ axis, and in the LTT phase, the octahedra rotate alternately about the $\langle 100\rangle$ axis. The angle δ of the rotations is about 0.05 rad in the LTO phase.[19] Let us first consider the LTO phase shown in Fig. 1(b). The $3d$ orbitals on the a (and b) Cu ion are given in the original coordinates by

$$|0\rangle=|x^2-y^2\rangle+\frac{\delta}{\sqrt{2}}(|yz\rangle-|zx\rangle)\ ,$$
$$|1\rangle=|3z^2-r^2\rangle+\delta(\tfrac{3}{2})^{1/2}(|yz\rangle+|zx\rangle)\ ,$$
$$|2\rangle=|yz\rangle-\frac{\delta}{\sqrt{2}}(|x^2-y^2\rangle+\sqrt{3}|3z^2-r^2\rangle-|xy\rangle)\ ,$$
$$|3\rangle=|zx\rangle-\frac{\delta}{\sqrt{2}}(-|x^2-y^2\rangle+\sqrt{3}|3z^2-r^2\rangle-|xy\rangle)\ , \tag{12}$$
$$|4\rangle=|xy\rangle-\frac{\delta}{\sqrt{2}}(|yz\rangle+|zx\rangle)\ ,$$

where δ should read $-\delta$ for the orbitals on the b ion. These expressions are used to obtain $\mathbf{L}_{jm0}$ of Eq. (6). The $2p$ orbitals on the kth oxygen ion are given with respect to the $x'y'z'$-coordinate system tilting with the tilt of the octahedron:

$$|p_x\rangle=|p_{x'}\rangle+\frac{\delta}{\sqrt{2}}|p_{z'}\rangle\ ,$$
$$|p_z\rangle=|p_{x'}\rangle-\frac{\delta}{\sqrt{2}}(|p_{x'}\rangle+|p_{y'}\rangle)\ , \tag{13}$$
$$|p_y\rangle=|p_{x'}\rangle+\frac{\delta}{\sqrt{2}}|p_{z'}\rangle\ .$$

These expressions are used to obtain $t_{jm,kn}$. Inserting the orbitals of Eqs. (12) and (13) into Eq. (9), we have the DM vector between the a and b ions of Fig. 1(b) as

$$\mathbf{D}_{ab}=(0,d_{\mathrm{LTO}},0)\ , \tag{14}$$
$$\mathbf{D}_{ac}=(-d_{\mathrm{LTO}},0,0)\ , \tag{15}$$

with

$$d_{\mathrm{LTO}}=\frac{4\sqrt{2}\delta\lambda}{\varepsilon_{zx}}t_{zx,p_z}(t_{x^2-y^2})^3\times\left[\frac{1}{\varepsilon_{p_\sigma}^2}\left[\frac{1}{2\varepsilon_{p_\sigma}}+\frac{1}{U}\right]+\frac{1}{U\varepsilon_{p_\sigma}\varepsilon_{p_z}}+\left[\frac{1}{\varepsilon_{p_\sigma}}+\frac{1}{\varepsilon_{p_z}}\right]^2\frac{1}{\varepsilon_{p_\sigma}+\varepsilon_{p_z}}\right], \tag{16}$$

where we have used the relation $\varepsilon_{yz}=\varepsilon_{zx}$. ε_{p_σ} is the ener-

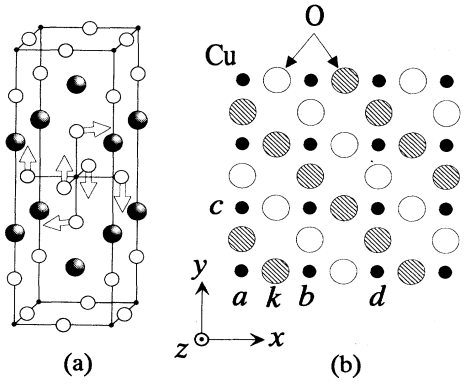

FIG. 1. (a) La_2CuO_4-type crystal structure in the LTO phase. Open arrows indicate the rotation of the CuO_6 octahedron. (b) The CuO_2 plane of the LTO phase. Oxygen ions indicated by an open (hatched) circle are tilted up (down) out of the plane.

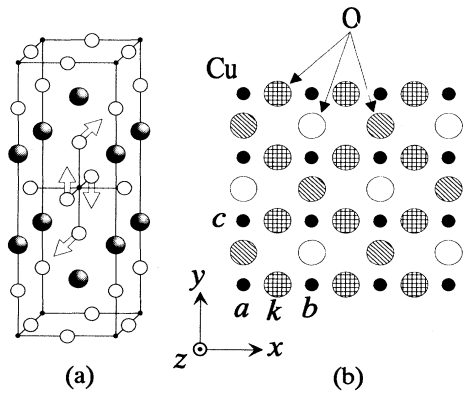

FIG. 2. As in Fig. 1, but for the LTT phase. In (b) oxygen ions indicated by a checked circle remain in the plane.

gy of the $2p_\sigma$ orbital, and t_{zx,p_z} is defined as the transfer of a hole between the Cu zx orbital and O $2p_z$ orbital. It should be noted that the symmetry relations[13] required by the crystal structure exactly hold in our expressions. In the LTT phase, the orbitals on the a (and b) Cu ion in Fig. 2(b) are written as

$$\begin{aligned}
&|0\rangle = |x^2-y^2\rangle + \delta|yz\rangle \ , \\
&|1\rangle = |3z^2-r^2\rangle + \delta\sqrt{3}|yz\rangle \ , \\
&|2\rangle = |yz\rangle - \delta(|x^2-y^2\rangle + \sqrt{3}|3z^2-r^2\rangle) \ , \\
&|3\rangle = |zx\rangle + \delta|xy\rangle \ , \\
&|4\rangle = |xy\rangle - \delta|zx\rangle \ ,
\end{aligned} \tag{17}$$

where δ should read $-\delta$ for the orbitals on the b ion. The $2p$ orbitals are written

$$\begin{aligned}
&|p_x\rangle = |p_{x'}\rangle \ , \\
&|p_z\rangle = |p_{x'}\rangle - \delta|p_{y'}\rangle \ , \\
&|p_y\rangle = |p_{x'}\rangle + \delta|p_{z'}\rangle \ .
\end{aligned} \tag{18}$$

Inserting these orbitals into Eq. (9), we have

$$\mathbf{D}_{ab} = (0,0,0) \tag{19}$$

and

$$\mathbf{D}_{ac} = (d_{\mathrm{LTT}},0,0) \ , \tag{20}$$

with

$$d_{\mathrm{LTT}} = \sqrt{2} d_{\mathrm{LTO}} \ . \tag{21}$$

These are the DM interactions in the CuO_2 plane of the LTO and LTT phases.

It may be useful to give a limiting case where only the oxygen $2p_\sigma$ orbital is taken into account. The Hamiltonian in this case is obtained by retaining only the $2p_\sigma$ orbital in Eqs. (7)–(11). We then readily confirm that the relation

$$\overleftrightarrow{\Gamma}_{ij} = \frac{1}{4J}(2\overleftarrow{\mathbf{D}}_{ij}\vec{\mathbf{D}}_{ij} - \overleftrightarrow{1}|\mathbf{D}_{ij}|^2) \tag{22}$$

holds between the J, $\mathbf{D}_{ij}$, and $\overleftrightarrow{\Gamma}_{ij}$ terms. Thus the Hamiltonian in the presence of only the single orbital on ligand oxygen ions becomes equivalent to the Moriya's spin Hamiltonian,[5] which is isotropic, as has been pointed out in Ref. 16.

Shekhtman, Entin-Wohlman, and Aharony[16] have pointed out for the single-band Hubbard model and also for the d-p model that the spin-orbit interaction cannot provide the anisotropic exchange interaction in a single bond connecting between two spins on the neighboring Cu sites. However, when one considers the anisotropy caused by the reduction of the crystal symmetry, it is of essential importance to take into account the contribution from multiorbitals of oxygen ions appearing due to lattice distortion. The Hamiltonian (5) leads to the anisotropic superexchange interaction even between the single Cu–O–Cu bond, as we can easily see from the Hamiltonian; it can be isotropic only when $\mathbf{C}_{jkn}/t_{j0,kn}$ is independent of n. In the case of La_2CuO_4-type crystals, the anisotropic superexchange interaction is the one that gives the weak ferromagnetism between the two spins of the neighboring a and b Cu ions, in both LTO and LTT phases.

III. MAGNETIC STRUCTURE IN THE INSULATING CuO_2 PLANE

In this section we examine the mechanism of the weak ferromagnetism of LTO-phase La_2CuO_4 and discuss a possible magnetism of La_2CuO_4-type crystals in the LTT phase. We examine the spin system on the two-dimensional square lattice, for which the Hamiltonian is given by Eq. (7). We assume that $\varepsilon_{p_\sigma} = \varepsilon_{p_z}$ for simplicity. This assumption does not change the essential physics discussed below. We then have the Hamiltonian

$$\begin{aligned}
H_{\mathrm{ex}} = J \sum_{\langle ij \rangle} \mathbf{S}_i \cdot \mathbf{S}_j \\
+ (1+\xi) \Bigg[\sum_{\langle ij \rangle} \mathbf{D}_{ij} \cdot (\mathbf{S}_i \times \mathbf{S}_j) \\
+ \frac{1}{4J} \sum_{\langle ij \rangle} \mathbf{S}_i (2\overleftarrow{\mathbf{D}}_{ij}\vec{\mathbf{D}}_{ij} - \overleftrightarrow{1}|\mathbf{D}_{ij}|^2)\mathbf{S}_j \Bigg] \ ,
\end{aligned} \tag{23}$$

with

$$\xi = \frac{\frac{1}{2}(3/2\varepsilon_{p_\sigma}^3)}{(1/\varepsilon_{p_\sigma}^2)(1/U + 1/2\varepsilon_{p_\sigma})} \ . \tag{24}$$

The contribution from the $2p_z$ orbital can be represented by a single parameter ξ owing to the above assumption: $\xi = 0$ gives the isotropic single bond, where only the p_σ orbitals are involved. ξ takes a value of ~ 1 for the realistic parameter values of U and ε_{p_σ}.

The DM vectors must have a spatial structure adapted to the crystal symmetry as shown in Fig. 3.[13] We define the angle of the DM vector θ in the LTO phase and the

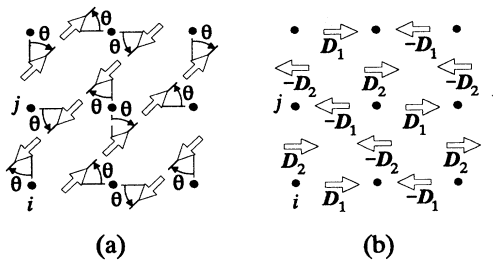

FIG. 3. Spatial structure of the DM vectors $\mathbf{D}_{ij}$ (indicated by open arrows) in the CuO_2 plane of (a) the LTO and (b) LTT phases. The arrows for the DM vectors are drawn by noting that the site j is always in the right or upper direction of the site i. The DM vectors always lie in the CuO_2 plane. In (a) the angle θ indicates the symmetry-permitted rotation of the DM vectors. In (b) the ratio D_2/D_1 is arbitrary, where $\mathbf{D}_1 = (D_1,0,0)$ and $\mathbf{D}_2 = (D_2,0,0)$.

ratio D_1/D_2 in the LTT phase (see Fig. 3). The symmetry arguments alone do not determine the values of θ and D_1/D_2. To examine what types of magnetism the spin-orbit interaction induces, we consider the Hamiltonian with a wide range of the parameter values.

We employ the exact-diagonalization technique for the finite-size 4×4 lattice with the periodic boundary condition. Note that the Hamiltonian does not commute with the total-spin operator, and we have to work with the 2^N spin space, where N is the number of sites. Translational symmetry is used to reduce the size of the Hilbert space. The ground-state energy and eigenstates are calculated by the Lanczos method[20] at the independent $\mathbf{k}$ points in the irreducible part of the Brillouin zone (see Fig. 4). Hereafter we refer to the $\mathbf{k}$ points in the Brillouin zone defined for the HTT structure without magnetic orderings.

To examine ground-state magnetic structures, we calculate the correlation functions

$$\kappa=\frac{1}{N^2}\left\langle\left[\sum_i S_i^z\right]^2\right\rangle , \tag{25}$$

for a measure of the uniform magnetization, and

$$\langle S_A^\alpha(-\mathbf{q})S_A^\alpha(\mathbf{q})\rangle=\left[\frac{2}{N}\right]^2\sum_{ij\in A}e^{i\mathbf{q}\cdot(\mathbf{R}_j-\mathbf{R}_i)}\langle S_i^\alpha S_j^\alpha\rangle , \tag{26}$$

at $\mathbf{q}=(0,0)$, for a measure of the uniaxial anisotropy. The summation in Eq. (26) runs over the sites on one of the two sublattices A. The ground state always has the wave vector $\mathbf{k}=(0,0)$, irrespective of the parameter values for both LTO and LTT phases.

Let us consider the LTO phase first. We have a frustrated spin system. The frustration is characterized by θ: The system is unfrustrated only at $\theta=-\pi/4$ and is most strongly frustrated at $\theta=\pi/4$. The expressions in Eqs. (14)–(16) give $\theta=\pi/2$. What is the spin structure in this case? The calculated results for the correlation function κ are shown in Fig. 5. First, we examine the case of $\xi=0$. κ is plotted as a function of θ in Fig. 5(a), which gives us a measure of the frustration. κ has a peak at $\theta=-\pi/4$ when D/J is small. The peak splits into two as D/J increases. Shekhtman, Entin-Wohlman, and Aharony[16] argued that the Hamiltonian (23) is isotropic at $\theta=-\pi/4$ and that frustration is essential for the emergence of weak ferromagnetism. In fact, $\langle S_A^\alpha(-\mathbf{q})S_A^\alpha(\mathbf{q})\rangle$ at $\theta=-\pi/4$ is independent of D/J, having the same value as that of the Heisenberg model, and also the ground-state energy is equivalent to that of the Heisenberg model with replacing J by $J+D^2/4J$. We thus confirm that the interaction between the spins is really isotropic; i.e., weak ferromagnetism is not induced at $\theta=-\pi/4$. It is also true that, for unrealistically large values of D/J, frustration generates the peaks in κ at $\theta\neq-\pi/4$, as shown in Fig. 5(a). However, for realistic values of D/J, frustration diminishes κ as θ changes from $-\pi/4$. Frustration seems not sufficient for weak ferromagnetism. What then is the true origin of weak ferromagnetism? It is straightforward to answer this question if we examine the behavior of κ at $\xi\neq0$. Figure 5(b), which shows the dramatic enhancement of κ, clearly indicates that the contribution from the $2p_z$ orbitals is essential for the emergence of weak ferromagnetism.

Next, we consider the LTT phase. It is characteristic of the LTT phase that all the DM vectors are along the x axis. The calculated result for the correlation functions (25) and (26) at $\xi=0$ is shown in Figs. 6(a) and 6(b). The LTT phase with $D_1/D_2=1$ corresponds to the LTO phase with $\theta=-\pi/4$. Thus the Hamiltonian is isotropic at $D_1/D_2=1$. When $D_1/D_2\neq1$, the four classical spins in a plaquette of the square lattice are of the antiferromagnetic arrangement with the anisotropy of the x direction in the ground state, of which the energy eigenvalue is $-\frac{1}{4}[2J+(D_1^2+D_2^2)/4J]$. Thus we understand Figs. 6(a) and 6(b) to indicate that the quantum spin system has the uniaxial anisotropy of the x direction in this case. Now let us examine the case at $\xi\neq0$, i.e., the effect of the $2p_z$

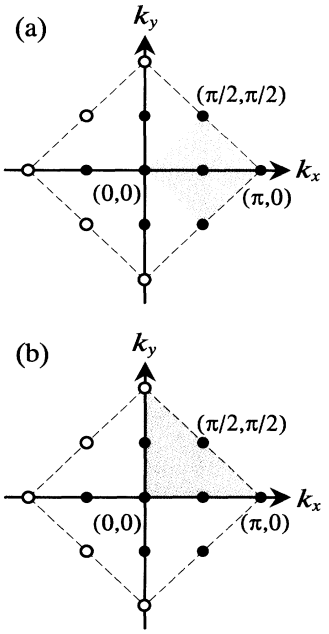

FIG. 4. Brillouin zone and its irreducible part (shaded) of the two-dimensional CuO_2 plane in (a) the LTO and (b) LTT phases. We take the axes k_x and k_y defined in the HTT phase.

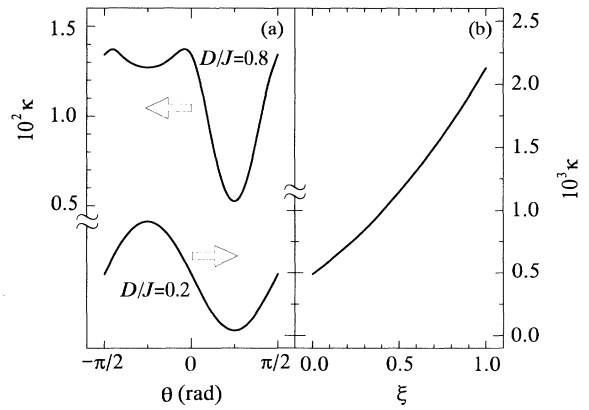

FIG. 5. (a) Correlation function κ as a function of θ at $\xi=0$. (b) The correlation function κ as a function of ξ at $\theta=-\pi/4$.

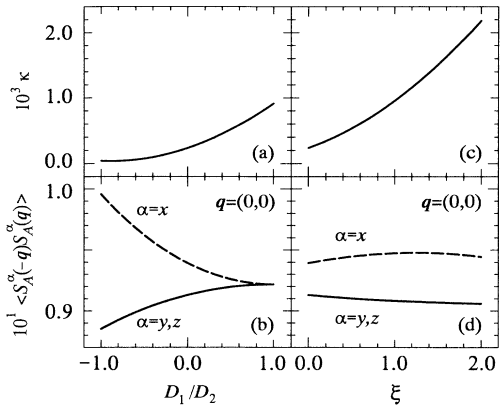

FIG. 6. (a) Correlation function κ as a function of D_1/D_2 at $\xi=0$. (b) The correlation function Eq. (26) at $\mathbf{q}=(0,0)$ as a function of D_1/D_2 at $\xi=0$. (c) The correlation function κ as a function of ξ at $D_1/D_2=0$. (d) The correlation function Eq. (26) at $\mathbf{q}=(0,0)$ as a function of ξ at $D_1/D_2=0$.

orbitals. In Figs. 6(c) and 6(d), we show the calculated results for the correlation functions (25) and (26) at $D_1/D_2=0$ as a function of ξ. The anisotropy along the x axis decreases for $\xi \gtrsim 1$, while κ increases monotonously with ξ. This behavior may be understood in the classical spin system: We find that the four classical spins in a plaquette of the square lattice have a ground state characterized by uniaxial antiferromagnetism for $\xi<1$ and by weak ferromagnetism for $\xi>1$. Thus, in the LTT phase, either uniaxial antiferromagnetism or weak ferromagnetism may be induced depending on how the oxygen $2p_z$ orbital contributes to the anisotropic superexchange interaction of the single Cu–O–Cu bond. A recent experiment has shown that weak ferromagnetism is induced in LTT-phase $La_{1.65}Nd_{0.35}CuO_4$.[21] The magnetic structures which we have obtained for La_2CuO_4-type crystals are illustrated in Fig. 7.

One of the characteristics of the spin-orbit interaction observable in the experiment is the magnetic anisotropy. The anisotropy has the following features in the realistic parameter region. In the LTO phase, the easy axis of magnetization cannot be in the $\langle 1\bar{1}0 \rangle$ direction, irrespective of whether weak ferromagnetism or uniaxial antiferromagnetism is obtained. In the LTT phase, the easy axis is always in the $\langle 100 \rangle$ direction. It has been observed[22] that in the LTO phase of La_2NiO_4 the antiferromagnetic easy axis is in the $\langle 1\bar{1}0 \rangle$ direction, unlike the case of La_2CuO_4 where it is in the $\langle 110 \rangle$ direction. As above, the spin-orbit interaction cannot provide such an anisotropy; the magnetic structure in the LTO phase of La_2NiO_4 must be of a different origin, say, the on-site anisotropy due to the Ni^{2+} ion of the spin of $S=1$.

IV. ELECTRONIC STRUCTURE IN THE DOPED CuO_2 PLANE

In the previous section, we have found that the magnetic structure depends on lattice distortion through the spin-orbit interaction. Recently, Bonesteel, Rice, and Zhang[15] have suggested that the spin-orbit interaction also results in a change of the electronic structure of hole-doped La_2CuO_4. Following Bonesteel, Rice, and Zhang,[15] we assume that the single-band Hubbard model should describe the relevant electronic structure of the CuO_2 plane. This is purely an assumption, because the multiband nature is expected to be important as we have shown for the magnetic structure in the previous sections. We believe, however, that it is necessary to examine the effect of the spin-orbit interaction within the single-band Hubbard model as a first step. Here we derive the effective Hamiltonian for the electronic structure as an extension of the t-J model. We then calculate the ground-state energy and photoemission spectrum by the exact-diagonalization technique. The effect of the lattice distortion via the spin-orbit interaction on the dynamics of a hole is thereby discussed. We confine ourselves to the LTT phase, which is interesting in relation to the anomalous properties in $La_{2-x}Ba_xCuO_4$.

Let us first write the Hamiltonian,

$$H=H_t+H_U+H_{LS} , \tag{27}$$

with

$$H_t=\sum_{\langle ij\rangle\sigma}\sum_{mn}(t_{im,jn}d^\dagger_{im\sigma}d_{jn\sigma}+\text{H.c.}) , \tag{28}$$

$$H_U=U\sum_{imn}d^\dagger_{im\uparrow}d_{im\uparrow}d^\dagger_{in\downarrow}d_{in\downarrow} \tag{29}$$

and

$$H_{LS}=\lambda\sum_i \mathbf{L}_i\cdot\mathbf{S}_i , \tag{30}$$

where $t_{im,jn}$ denotes the transfer of holes between m and n orbitals on the neighboring i and j sites. The other notation is the same as those in Eqs. (2)–(4). As has been done in Sec. II, we obtain the effective Hamiltonian by eliminating the excited crystal-field levels:

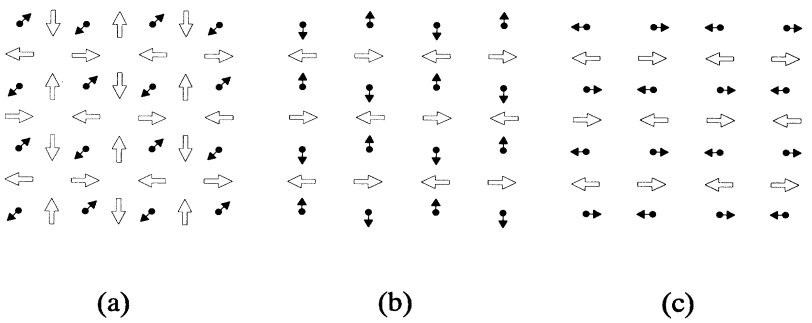

FIG. 7. Schematic representation of the spin structure (solid arrows) and direction of the DM vectors (open arrows) in the CuO_2 plane of the LTO and LTT phases. (a) Weak ferromagnetism in the LTO phase. All the spins cant up out of the plane. The easy axis is in the $\langle 110 \rangle$ direction. (b) Weak ferromagnetism in the LTT phase. All the spins cant up out of the plane. The easy axis is on the (100) plane. (c) Uniaxial antiferromagnetism in the LTT phase. The easy axis is in the $\langle 100 \rangle$ direction.

$$H=\sum_{\langle ij\rangle\sigma}(t_{i0,j0}d^{\dagger}_{i0\sigma}d_{j0\sigma}+\text{H.c.})+\sum_{\langle ij\rangle}\sum_{\alpha\beta}[\mathbf{C}_{ij}\cdot(d^{\dagger}_{i0\alpha}\boldsymbol{\sigma}_{\alpha\beta}d_{j0\beta})+\text{H.c.}]+U\sum_{i}n_{i\uparrow}n_{i\downarrow}\ , \tag{31}$$

with

$$\mathbf{C}_{ij}=-\frac{\lambda}{2}\left[\sum_{m}\frac{\mathbf{L}^{*}_{im0}}{\varepsilon_m}t_{im,j0}+\sum_{m}\frac{\mathbf{L}_{jm0}}{\varepsilon_m}t_{i0,jm}\right]\ , \tag{32}$$

where $n_{i\sigma}=d^{\dagger}_{i0\sigma}d_{i0\sigma}$. We apply the second-order perturbation with respect to the transfer parameters in Eq. (31) and obtain the effective Hamiltonian

$$H_{\text{eff}}=H_{t\text{-}J}+H_{\text{s.o.}}\ , \tag{33}$$

with

$$H_{t\text{-}J}=-t\sum_{\langle ij\rangle\sigma}(c^{\dagger}_{i\sigma}c_{j\sigma}+\text{H.c.})+J\sum_{\langle ij\rangle}(\mathbf{S}_i\cdot\mathbf{S}_j-\tfrac{1}{4}n_in_j) \tag{34}$$

and

$$H_{\text{s.o.}}=\sum_{\langle ij\rangle}\sum_{\alpha\beta}[\mathbf{C}_{ij}\cdot(c^{\dagger}_{i\alpha}\boldsymbol{\sigma}_{\alpha\beta}c_{j\beta})+\text{H.c.}]+\sum_{\langle ij\rangle}\mathbf{D}_{ij}\cdot(\mathbf{S}_i\times\mathbf{S}_j)+\sum_{\langle ij\rangle}\left[\mathbf{S}_i\overleftrightarrow{\Gamma}_{ij}\mathbf{S}_j-\frac{1}{4}\left[\frac{|\mathbf{D}_{ij}|^2}{4J}\right]n_in_j\right]\ , \tag{35}$$

where

$$c^{\dagger}_{i\sigma}=(1-n_{i-\sigma})d^{\dagger}_{i0\sigma}\ , \tag{36}$$

$$J=\frac{4t^2}{U}\ , \tag{37}$$

$$\mathbf{D}_{ij}=\frac{4it}{U}(\mathbf{C}_{ij}-\mathbf{C}_{ji})=2i(J/t)\mathbf{C}_{ij}\ , \tag{38}$$

and

$$\overleftrightarrow{\Gamma}_{ij}=\frac{4}{U}[\overleftrightarrow{\mathbf{C}}_{ij}\vec{\mathbf{C}}_{ji}+\overleftrightarrow{\mathbf{C}}_{ji}\vec{\mathbf{C}}_{ij}+\overleftrightarrow{1}(\mathbf{C}_{ij}\cdot\mathbf{C}_{ji})]=\frac{J}{t^2}[\overleftrightarrow{\mathbf{C}}_{ij}\vec{\mathbf{C}}_{ji}+\overleftrightarrow{\mathbf{C}}_{ji}\vec{\mathbf{C}}_{ij}+\overleftrightarrow{1}(\mathbf{C}_{ij}\cdot\mathbf{C}_{ji})]\ . \tag{39}$$

We have used an abbreviation $t=-|t_{i0,j0}|$. The pair-hopping term has been neglected. The Hamiltonian (33) is an extension of the so-called t-J model, which includes the effect of the spin-orbit interaction. Note that the spin-orbit interaction induces the hopping term with an effective vector potential (or flux).[14,15] We call the first term of Eq. (35) the spin-orbit hopping term.

Inserting the orbitals of Eqs. (12), (13), and (17), and (18) into Eq. (32), we have

$$\mathbf{C}_{ab}=i(c_x,c_y,0) \tag{40}$$

and

$$\mathbf{C}_{ac}=-i(c_y,c_x,0)\ , \tag{41}$$

with

$$c_x=\frac{\lambda\delta}{\sqrt{2}\varepsilon_{yz}}(t_{yz,yz}+t_{x^2-y^2,x^2-y^2}+\sqrt{3}t_{3z^2-r^2,x^2-y^2}) \tag{42}$$

and

$$c_y=-\frac{\lambda\delta}{\sqrt{2}\varepsilon_{yz}}(t_{yz,yz}+t_{x^2-y^2,x^2-y^2}-\sqrt{3}t_{3z^2-r^2,x^2-y^2})\ , \tag{43}$$

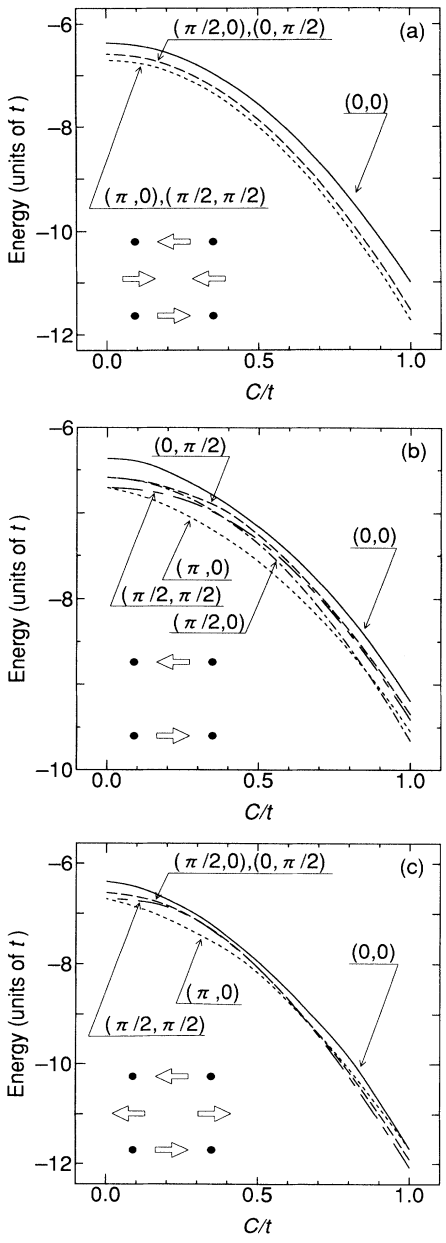

FIG. 8. Calculated energy eigenvalues of H_{eff} as a function of $C/t=D/2J$. The results are for the 16-site square lattice with a hole at $J=0.25t$. (a), (b), and (c) correspond, respectively, to the case where $D_2/D_1=1$, 0, and -1 in the LTT phase as shown in the insets.

for the LTO phase, and

$$\mathbf{C}_{ab}=i(c_x',0,0) \tag{44}$$

and

$$\mathbf{C}_{ac}=i(c_x'',0,0)\ , \tag{45}$$

with

$$c_x'=\frac{\lambda\delta}{\varepsilon_{yz}}(t_{yz,yz}+t_{x^2-y^2,x^2-y^2}+\sqrt{3}t_{3z^2-r^2,x^2-y^2}) \tag{46}$$

and

$$c_x''=\frac{\lambda\delta}{\varepsilon_{yz}}(-t_{yz,yz}+t_{x^2-y^2,x^2-y^2}-\sqrt{3}t_{3z^2-r^2,x^2-y^2})\ , \tag{47}$$

for the LTT phase. We note that $t=t_{x^2-y^2,x^2-y^2}$ in Eqs. (34) and (37)–(39). $t_{\eta,\zeta}$ denotes the transfer between the neighboring η and ζ orbitals. The corresponding expressions for $\mathbf{D}_{ij}$ and $\vec{\Gamma}_{ij}$ are given by using Eqs. (38) and (39).

In the following we calculate the ground-state energy and photoemission spectrum for the above Hamiltonian and examine the effect of lattice distortion on the dynamics of a hole through the spin-orbit interaction. We apply the exact-diagonalization technique for the 4×4 square lattice with the periodic boundary condition. The spin quantization axis is taken along the DM vectors in the LTT phase, so that we may have the Hamiltonian commutable with the component (along the spin quantization axis) of the total-spin operator. As we have argued in Sec. III, we do not take the expressions of Eqs. (42), (43), (46), and (47) seriously, but rather change the parameter values over a wide range within the symmetry constraint and Eqs. (38) and (39). We take the relation $D/J=2C/t$, where $D=|\mathbf{D}_{ij}|$, $C=|\mathbf{C}_{ij}|$.

The calculated results for the ground-state energy at a number of wave vectors are shown in Figs. 8(a), 8(b), and 8(c). Figure 8(a) is the result for $D_2/D_1=1$, which corresponds to the case where there is no frustration. Here the Hamiltonian can be mapped onto the isotropic exchange Hamiltonian when there is no hole. It is found that the energy eigenvalues obtained are identical with those of the t-J model if we replace t by $t[1+(C/t)^2]^{1/2}$ and J by $J[1+(C/t)^2]$. Thus the system with a hole at $D_2/D_1=1$ is exactly equivalent to the t-J model. Figure 8(b) is the result for $D_2/D_1=0$. The energies are not degenerate. With increasing C/t, the ground-state wave vector changes from $\mathbf{k}=(\pi,0)$ for $C/t\lesssim0.85$ to $\mathbf{k}=(\pi/2,0)$ for $C/t\gtrsim0.85$. Figure 8(c) is the result for $D_2/D_1=-1$, which corresponds to the case where uniaxial antiferromagnetism is most strongly induced when there is no hole. Here the energies at $\mathbf{k}=(\pi/2,0)$ and $(0,\pi/2)$ are degenerate because the Hamiltonian at $D_2/D_1=-1$ in the LTT phase is equivalent to the Hamiltonian at $\theta=\pi/4$ in the LTO phase and the wave vectors $(\pi/2,0)$ and $(0,\pi/2)$ belong to the same star of $\mathbf{k}$ in the LTO phase. With increasing C/t, the ground-state wave vector changes from $\mathbf{k}=(\pi,0)$ for $C/t\lesssim0.7$ to $\mathbf{k}=(\pi/2,\pi/2)$ for $C/t\gtrsim0.7$.

We find in the LTT phase that, by changing D_2/D_1 from 1 to -1 with fixing D_1, the degeneracy between $(\pi/2,\pi/2)$ and $(\pi,0)$ is lifted monotonously to make $(\pi,0)$ the ground-state wave vector. The level separation increases linearly with respect to C/t when $D_2/D_1\neq1$ and C/t is small. The effect of lattice distortion emerging via the spin-orbit coupling is, therefore, to lower the energy at $\mathbf{k}=(\pi,0)$ compared with $\mathbf{k}=(\pi/2,\pi/2)$. This effect is the largest when the uniaxial antiferromagnetic character appears most strongly in the undoped systems.

The change in the symmetry of the ground state may also be seen in the calculated photoemission spectral densities $I(\mathbf{k},\omega)$ for the undoped system. We calculate

$$I(\mathbf{k},\omega)=-\frac{1}{\pi}\sum_{\sigma}\mathrm{Im}\left\langle \mathrm{g.s.}\left|c_{\mathbf{k}\sigma}^{\dagger}\frac{1}{\omega-H_{\mathrm{eff}}+\varepsilon_{\mathrm{g.s.}}+i\eta}c_{\mathbf{k}\sigma}\right|\mathrm{g.s.}\right\rangle \tag{48}$$

and

$$I(\omega)=\sum_{\mathbf{k}}I(\mathbf{k},\omega)\ , \tag{49}$$

where $\varepsilon_{\mathrm{g.s.}}$ and $|\mathrm{g.s.}\rangle$ are the ground-state energy and eigenvector of the undoped system, and $c_{\mathbf{k}\sigma}$ is the Fourier transform of the projected annihilation operator $c_{i\sigma}$. η is a small parameter which gives a finite width to the δ functions appearing at each pole of $I(\omega)$. We use the Lanczos algorithm[23] for the numerical calculation. The results for $I(\mathbf{k},\omega)$ at $\mathbf{k}=(\pi/2,\pi/2)$ and $(\pi,0)$ with $C/t=0.1$ are shown in Fig. 9. We see a peak at $\omega\simeq-1.9$ when $D_2/D_1=1$. With changing D_2/D_1 from 1 to -1, the peak at $\mathbf{k}=(\pi/2,\pi/2)$ remains as a single peak, but the peak at $\mathbf{k}=(\pi,0)$ splits into two peaks and a small peak appears at $\omega\simeq-1.73$. The lowest-energy peak at $\mathbf{k}=(\pi,0)$ is lower than the lowest-energy peak at $\mathbf{k}=(\pi/2,\pi/2)$, whose energy difference corresponds to the splitting of the one-hole energy levels described above.

It has been argued[24] that the one-hole ground state of the t-J model in the infinite system is at the wave vector $\mathbf{k}=(\pi/2,\pi/2)$. We have shown here that the effect of lattice distortion lowers the energy of $\mathbf{k}=(\pi,0)$ through the spin-orbit coupling. Is this effect large enough to change the ground-state wave vector? It has been reported[24] that the energy-level difference between $\mathbf{k}=(\pi/2,\pi/2)$ and $(\pi,0)$ in the t-J model is an order of $J/10$ in units of t. We can evaluate the parameter values for La_2CuO_4: $\delta\simeq0.05$ rad,[19] $\lambda\simeq0.1$ eV,[25] $\varepsilon_{yz}\simeq1$ eV,[26] and $t_{x^2-y^2,x^2-y^2}\simeq0.4$ eV.[26] Then we have $C\simeq0.003$ eV. This value is two orders of magnitude smaller than the value of $t=0.4$ eV.[26] In Fig. 8(c), where we see the strongest effect of lowering the energy of $\mathbf{k}=(\pi,0)$, we

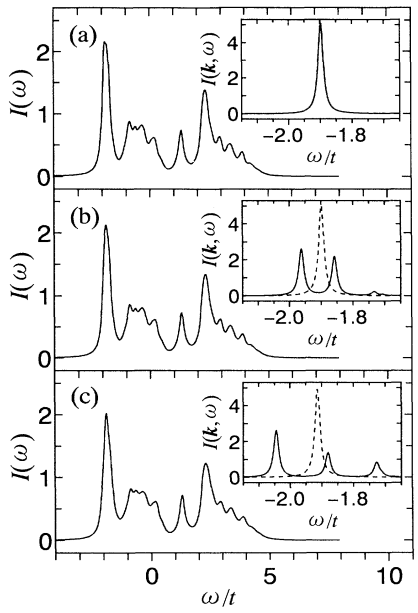

FIG. 9. Calculated spectral densities $I(\omega)$ for H_{eff} at $C/t=0.1$. A broadening of $\eta=0.1t$ is used. (a), (b), and (c) correspond, respectively, to the case where $D_2/D_1=1$, 0, and -1 in the LTT phase. $I(\mathbf{k},\omega)$ at $\mathbf{k}=(\pi,0)$ (solid curve) and $(\pi/2,\pi/2)$ (dashed curve) is shown in the insets of panels (a), (b), and (c). In (a) the two curves coincide. A broadening of $\eta=0.01t$ is used.

find that the energy-level splitting between $\mathbf{k}=(\pi/2,\pi/2)$ and $(\pi,0)$ at $C/t\simeq 0.01$ is $\sim 0.01t$. This is less than a half of the value of $J/10=0.025t$. We therefore conclude that the effect of lattice distortion via the spin-orbit coupling is too small to change the ground-state wave vector $\mathbf{k}=(\pi/2,\pi/2)$ into $(\pi,0)$.

Here we have examined the spin-orbit effect starting with the single-band Hubbard model. The extended t-J model is not, however, a sufficient model for describing the distorted CuO_2 plane with the spin-orbit interaction, as we have stated in the beginning of this section. In future work we should work out how the spin-orbit term arises in the process of deriving a proper single-band model that describes the multiband nature of the CuO_2 plane.

V. CONCLUSIONS

We have examined the effect of the lattice distortion appearing through the spin-orbit coupling on the magnetic and electronic structures of the CuO_2 plane of La_2CuO_4-type crystals. The contribution of the $2p_z$ orbital of the in-plane oxygen ions is essential for understanding the magnetic structure; the DM interaction does not always induce weak ferromagnetism, but can provide a variety of magnetism. We have shown that, in the LTO phase of La_2CuO_4, the contribution from the $2p_z$ orbital is essential for the emergence of weak ferromagnetism. In the LTT phase, either uniaxial antiferromagnetism or weak ferromagnetism may be induced depending on how the oxygen $2p_z$ orbital contributes to the anisotropic superexchange interaction of the single Cu–O–Cu bond. The effect of the spin-orbit interaction on the dynamics of a hole has been studied within the extended t-J model, which includes both spin-orbit hopping and the DM interaction. We have shown that lattice distortion works to change the symmetry of the electronic ground state via the spin-orbit coupling. The effect is, however, small in the actual CuO_2 systems and seems irrelevant to the anomalous properties of $La_{1.88}Ba_{0.12}CuO_4$.

ACKNOWLEDGMENTS

We would like to thank Professor T. M. Rice for valuable discussions and communications, and Dr. N. E. Bonesteel for useful correspondence. This work was supported by Grants-in-Aid for Scientific Research on Priority Areas "Computational Physics as a New Frontier in Condensed Matter Research" and "Mechanism of Superconductivity" from the Ministry of Education, Science, and Culture of Japan.

[1]J. D. Axe, A. H. Moudden, D. Hohlwein, D. E. Cox, K. Mohanty, A. R. Moodenbaugh, and Y. Xu, Phys. Rev. Lett. **62**, 2751 (1989); J. D. Axe, D. E. Cox, K. Mohanty, H. Moudden, A. R. Moodenbaugh, Y. Xu, and T. R. Thurston, IBM J. Res. Dev. **33**, 382 (1989).

[2]M. K. Crawford, R. L. Harlow, E. M. McCarron, W. E. Fameth, J. D. Axe, H. Chou, and Q. Huang, Phys. Rev. B **44**, 7749 (1991).

[3]K. Fukuda, S. Shamoto, M. Sato, and K. Oka, Solid State Commun. **65**, 1323 (1988); T. Thio, T. R. Thurston, N. W. Preyer, P. J. Picone, M. A. Kastner, H. P. Jenssen, D. R. Gabbe, C. Y. Chen, R. J. Birgeneau, and A. Aharony, Phys. Rev. B **38**, 905 (1988); M. A. Kastner, R. J. Birgeneau, T. R. Thurston, P. J. Picone, H. P. Jenssen, D. R. Gabbe, M. Sato, K. Fukuda, S. Shamoto, Y. Endo, K. Yamada, and G. Shirane, *ibid.* **38**, 6636 (1988); T. Thio, C. Y. Chen, B. S. Freer, D. R. Gabbe, H. P. Jenssen, M. A. Kastner, P. J. Picone, N. W. Preyer, and R. J. Birgeneau, *ibid.* **41**, 231 (1990).

[4]I. E. Dzyaloshinski, J. Phys. Chem. Solids **4**, 241 (1958).

[5]T. Moriya, Phys. Rev. **120**, 91 (1960).

[6]A. R. Moodenbaugh, Y. Xu, M. Suenaga, T. J. Folkerts, and R. N. Shelton, Phys. Rev. B **38**, 4596 (1988).

[7]M. Sera, Y. Ando, S. Kondoh, K. Fukuda, M. Sato, I. Watanabe, S. Nakashima, and K. Kumagai, Solid State Commun. **69**, 851 (1989).

[8]Y. Maeno, A. Odagawa, N. Kakehi, T. Suzuki, and T. Fujita, Physica C **173**, 322 (1991).

[9]Y. Koike, N. Watanabe, T. Noji, and Y. Saito, Solid State Commun. **78**, 511 (1991).

[10]G. M. Luke, L. P. Le, B. J. Sternlieb, W. D. Wu, Y. J. Uemura, J. H. Brewer, T. M. Riseman, S. Ishibashi, and S. Uchida, Physica C **185-189**, 1175 (1991).

[11]N. Wada, Y. Nakamura, and K. Kumagai, Physica C **185-189**, 1177 (1991); I. Watanabe, K. Kawano, K. Kumagai, K. Nishiyama, and K. Nagamine, J. Phys. Soc. Jpn. **61**, 3058 (1992).

[12]H. Takagi, R. J. Cava, M. Marezio, B. Batlogg, J. J. Krajewski, W. F. Peck Jr., P. Bordet, and D. E. Cox, Phys. Rev.

Lett. **68**, 3777 (1992).
[13]D. Coffey, K. S. Bedell, and S. A. Trugman, Phys. Rev. B **42**, 6509 (1990).
[14]D. Coffey, T. M. Rice, and F. C. Zhang, Phys. Rev. B **44**, 10 112 (1991); **46**, 5884 (1992).
[15]N. E. Bonesteel, T. M. Rice, and F. C. Zhang, Phys. Rev. Lett. **68**, 2684 (1992).
[16]L. Shekhtman, O. Entin-Wohlman, and A. Aharony, Phys. Rev. Lett. **69**, 836 (1992); L. Shekhtman, A. Aharony, and O. Entin-Wohlman (unpublished).
[17]W. Koshibae, Y. Ohta, and S. Maekawa, Physica C **185-189**, 1509 (1991).
[18]N. E. Bonesteel, Phys. Rev. B (to be published).
[19]S-W. Cheong, J. D. Thompson, and Z. Fisk, Physica C **158**, 109 (1989).
[20]C. Lanczos, J. Res. Natl. Bur. Stand. **45**, 255 (1950).
[21]S. Shamoto, T. Kiyokura, M. Sato, K. Kakurai, Y. Nakamura, and S. Uchida, Physica C **203**, 7 (1992); B. Keimer, R. J. Birgeneau, A. Cassanho, Y. Endoh, M. Greven, M. A. Kastner, and G. Shirane (unpublished).
[22]G. Aeppli and D. J. Buttrey, Phys. Rev. Lett. **61**, 203 (1988); K. Yamada, T. Omata, K. Nakajima, S. Hosoya, T. Sumida, and Y. Endoh, Physica C **191**, 15 (1992).
[23]E. R. Gagliano and C. A. Balseiro, Phys. Rev. Lett. **59**, 2999 (1987).
[24]T. Itoh, M. Arai, and T. Fujiwara, Phys. Rev. B **42**, 4834 (1990); J. Inoue and S. Maekawa, J. Phys. Soc. Jpn. **59**, 2110 (1990).
[25]W. Low, in *Solid State Physics,* edited by F. Seitz and D. Turnbull (Academic, New York, 1960), Suppl. 2, p. 77.
[26]A. K. McMahan, R. M. Martin, and S. Satpathy, Phys. Rev. B **38**, 6650 (1988); M. S. Hybertsen, E. B. Stechel, M. Schluter, and D. R. Jennison, *ibid.* **41**, 11 068 (1990); S. B. Bacci, E. R. Gagliano, R. M. Martin, and J. F. Annett, *ibid.* **44**, 7504 (1991).